Ceramics-Silikáty 70 (1), 82-88 (2026)
www.ceramics-silikaty.cz doi: 10.13168/cs.2025.0053

INCREASING THE MODULUS OF A SODIUM SILICATE SOLUTION BY DISSOLVING POROUS SILICA POWDER

CHENGHONG WANG*, ZHONGYA LI*, **, #SHIQUAN LIU*, **

School of Materials Science and Engineering, Qilu University of Technology (Shandong Academy of Sciences), Jinan 250353, Shandong, PR China
Shandong Key Laboratory of Advanced Glass Manufacturing and Technology, Jinan 250353, Shandong, PR China

#E-mail: sqliu@qlu.edu.cn

Submitted September 6, 2025, accepted October 18, 2025

Keywords: Sodium silicate solution, Tuning modulus, Porous silica powder

Traditionally, increasing the modulus of water glass solution (soluble sodium silicate) requires increasing the silica content in batches, which are used to melt the binary Na_2O-SiO_2 glass precursor. This is only applicable for large-scale production and inevitably results in a high melting temperature and high energy consumption. Herein, porous silica powder was dissolved in a commercial water glass solution under moderate temperature heating condition. Thus, the modulus of the water glass solution was easily tuned from 3.06 to 3.87, providing a convenient way that is suitable for obtaining small quantities of water glass solution with a high modulus. The pH, density, viscosity and conductivity of the tuned solution were characterised in detail. The FTIR and ^{29}Si NMR spectroscopy evidenced that the porous silica dissolved in the water glass solution, but its [SiO_4] skeleton was largely preserved.

INTRODUCTION

Water glass, commonly known as soluble sodium silicate, is an inorganic compound with the chemical formula $Na_2O{\cdot}nSiO_2$ [1]. It is mainly produced by melting the mixture of sodium carbonate and quartz sand with an appropriate SiO_2/Na_2O molar ratio, mostly in the range of 2~3.6 at a high temperature of 1300-1400°C [2-4]. After the melt is quenched to form a glass frit, it can be transformed into water glass solutions under hydrothermal conditions [4-6]. Due to its adhesive, buffering and flocculating performance, water glass solutions are widely used in construction, casting, detergents and wastewater treatment [7-10].

The modulus "n" of water glass, which refers to the molar ratio of SiO_2 to Na_2O, is a key parameter that influences not only the glass melting temperature, but also the solubility, bonding strength, water resistance, and curing speed of water glass solutions when applied in different fields [11, 12]. Generally, high-modulus water glass is suitable for applications such as precision casting, the synthesis of acid-resistant materials and molecular sieves. The traditional industrial method for increasing the modulus of water glass involves increasing silica sand in batches to make Na_2O-SiO_2 binary glass. This inevitably raises the glass melting temperature, which significantly increases the energy consumption and cost of the water glass production [13, 14]. In addition, this method is applicable in the large-scale production of high-modulus solid water glass, but not suitable for small-scale synthesis, especially when a series of water glasses with different moduli are desired. Therefore, it is worthwhile to explore new methods that can easily tune the modulus of water glass.

This study proposes a method of increasing the modulus of water glass via a low-temperature facile route, in which porous silica powder was dissolved in commercial water glass solutions at low temperature. A series of water glass solutions with modulus ranges of 3.06-3.87 was obtained. In addition, the variation in the pH, density, viscosity, conductivity, as well as the structure of the tuned water glass solutions, was systematically studied.

EXPERIMENTAL

Raw materials and preparation procedures

Water glass solutions (SP38) with a modulus of 3.06 were purchased from URE Refractories (Jiashan, China). A porous silica with a Brunauer-Emmett-Teller (BET) surface area of 147 $m^2 \cdot g^{-1}$ and a pore volume of 0.885 $cm^3 \cdot g^{-1}$ was provided by a factory. The powder particles are spherical, sized 2~100 μm (Figure 1a). The spheres consisted of aggregated nanometre-sized grains (Figure 1b). A narrow and large hysteresis loop in its isotherm was at a relative pressure higher than 0.9 (Figure 1c), suggesting that the pores mainly originated from the inter-voids of the primary grains in the silica gel. All the materials were applied directly without further purification.

A series of water glass solutions were prepared as follows: First, 50 mL of water glass was diluted 1.3 times, into which a certain amount of silica powder was added. The mixture was then sealed and heated in a water bath at 80 °C under stirring for 1.5 h. After the mixture was cooled to room temperature, water glass solutions with increasing silica contents were obtained. The obtained samples were encoded as WG-Sx, the WG-S0.3, WG-S0.6, WG-S1, WG-S2, WG-S3, and WG-S4 samples, where "x" represents the amount of silica powder dissolved in the water solutions.

Characterisations

The modulus of the water glass solution was measured by determining the content of the Na and Si elements in the sample using Inductively coupled plasma emission spectroscopy (ICP, iCAP PRO XP, Thermo Scientific, USA). After converting the contents of Si and Na into the corresponding SiO_2 and Na_2O oxides, the modulus of water glass was obtained.

The structure of the water glass solutions was analysed using a Fourier transform infrared spectrometer with a resolution of 2 cm^{-1} (FTIR, ALPHA II, Bruker, Germany). The scan range was 4000 to 400 cm^{-1}. The Qn groups (Q^0, Q^1, Q^{2C}, Q^2, Q^3, and Q^4) of the [SiO_4] structural units were characterised using a nuclear magnetic resonance spectrometer (NMR, JNM-ECZL600M, JEOL, Japan). The pH of the tuned water glass was measured using a pH meter (Mettler Toledo, Switzerland). The density of the samples was measured using a density balance (MD-100-II, XUHUI XINRUI, China). A rapid viscometer was used to measure the viscosity of the prepared water glass solutions (RVA-TecMaster, Perten, Sweden). The conductivity was measured on a Zeta potential analyser (Zetasizer Nano ZS, Malvern Panalytical, England).

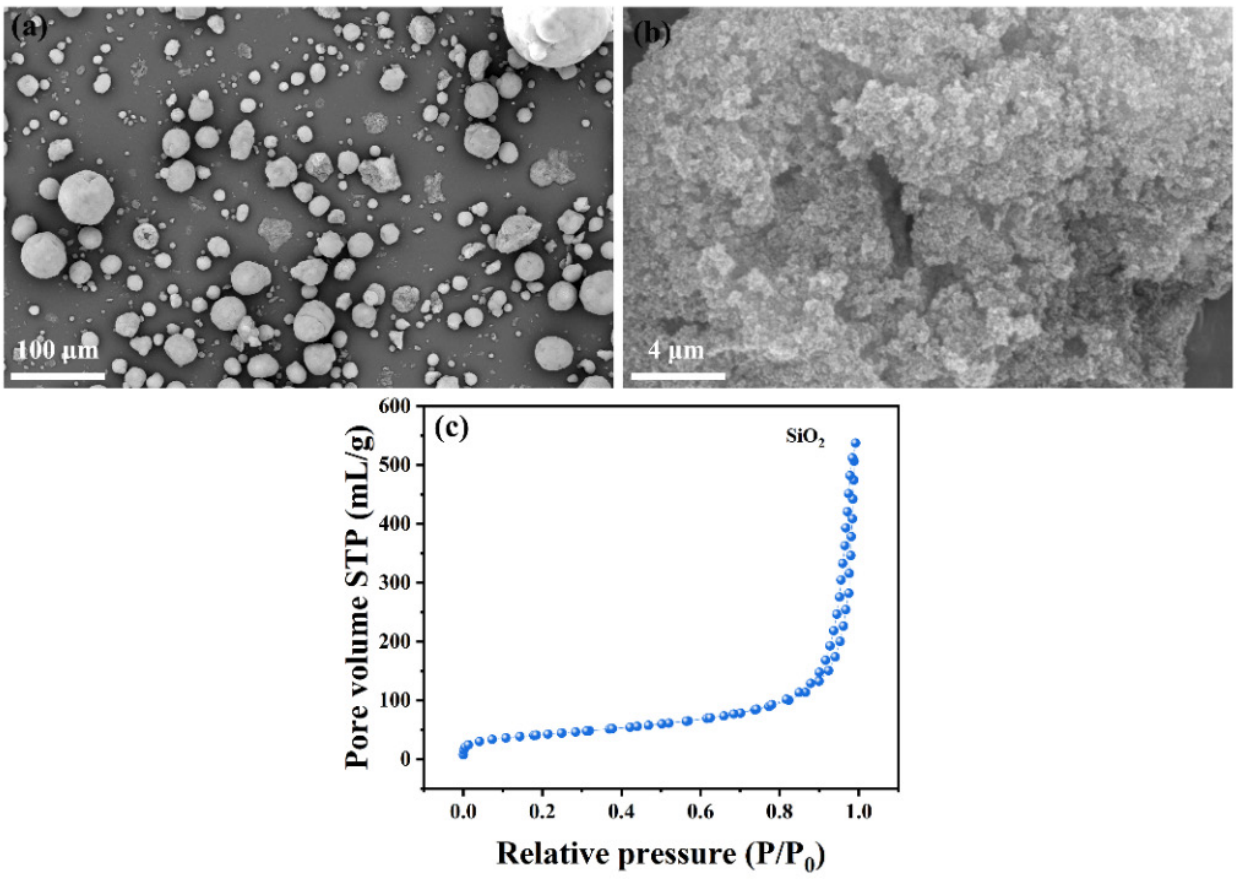

Figure 1. (a-b) SEM images and (c) N_2-sorption isotherm of the porous SiO_2 powder.

RESULTS AND DISCUSSIONS

Variation of the modulus and the properties of the prepared water glass solutions

Table 1 shows the amount of silica added for the synthesis of the WG-Sx water glass solutions. It is reasonable that the modulus of the water glass gradually increases with the addition of silica powder.

Table 1. The amount of SiO_2 powder added in the synthesis and the moduli of the obtained water glass solutions.

Sample number	The amount of SiO_2 powder added(g)	Modulus of water glass
WG	0	3.06
WG-S0.3	0.3	3.16
WG-S0.6	0.6	3.18
WG-S1	1	3.38
WG-S2	2	3.55
WG-S3	3	3.72
WG-S4	4	3.87

Figure 2a shows the pH values of the tuned water glass solutions with different moduli. The initial WG water glass solutions have a pH of 11.7. As the modulus increases, the pH value gradually decreases, which is attributed to the reaction between the added SiO_2 and hydroxide ions in the alkaline solution to generate silicate anions or $Si(OH)_4$, leading to a reduction in the hydroxide ion concentration in the solution and a corresponding decrease in alkalinity [15, 16].

As shown in Figure 2b, the increase in modulus resulted in an increase in the density of the tuned water glass. The addition of silica powder to the water glass increased the solute content per unit volume, thereby increasing the solution density. Meanwhile, the viscosity of the water glass rises from 36 cp to 85 cp when the modulus increases (Figure 2c). This is attributed to the increase in the SiO_2 content in the water glass, which strengthens the intermolecular forces and the siloxane network structure, leading to greater flow resistance and, consequently, to a higher viscosity [17, 18].

Figure 2d shows that the conductivity of the water glass solutions first slightly increases and then decreases with the increase in the modulus. When 1 g of SiO_2 is added, the WG-S1 water glass with a modulus of 3.38 achieves maximum conductivity (~40.8 $mS \cdot cm^{-1}$). This occurred because the number of ions in the water glass increased with the addition of the SiO_2 powder. However, further increasing the SiO_2 addition increases the viscosity of the water glass, impeding the ion migration and causing a continuous decrease in the conductivity rather than an increase [17].

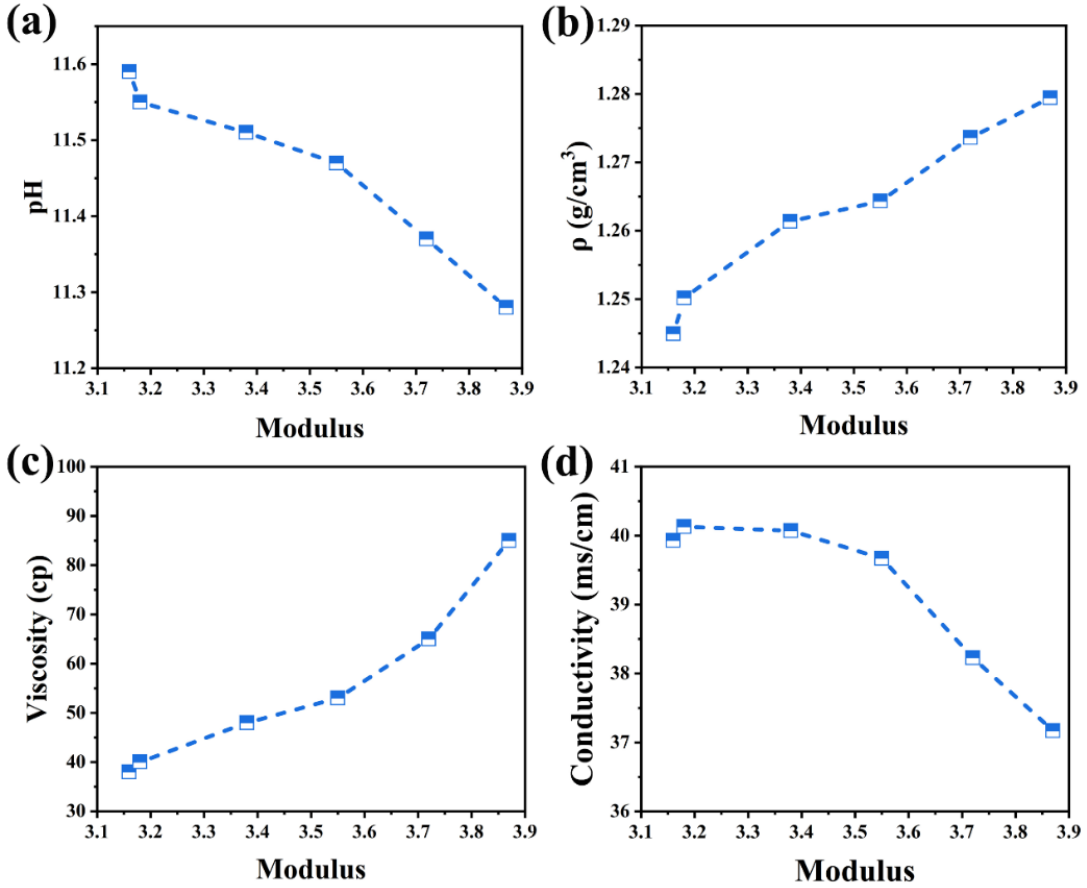

Figure 2. Variations in the pH (a), density (b), viscosity (c), and conductivity (d) of the tuned WG-Sx water glass solutions with the increasing modulus.

The structural characterisation of the tuned water glass solutions

The FTIR spectra of the tuned water glass solutions are compared (Figure 3). The main absorption bands are located at ~1130 cm^{-1}, ~1008 cm^{-1}, ~875 cm^{-1}, ~773 cm^{-1}, ~580 cm^{-1}, and ~420 cm^{-1} (Figure 3a), corresponding to the asymmetric stretching vibration of Si-O-Si/(H)O-Si--O(H), the stretching vibration of (Na)O-Si-O(Na), the bending vibration of Si-OH, the symmetric stretching vibration of Si-O-Si, the bending vibration of (Na)O-Si--O(Na), the bending vibration of Si-O-Si, respectively [19, 20]. Compared to precursor water glass solutions, the spectra of tuned water glass solutions do not show new absorption bands. Furthermore, as the modulus of water glass increases, the asymmetric stretching vibration absorption band of the O-Si-O bond near 1008 cm^{-1} shifts to a higher wave number at ~1029 cm^{-1}, accompanied by a broadening of the absorption band (Figure 3b), indicating the increased connectivity of the skeleton of [SiO_4] in the water glass solutions.

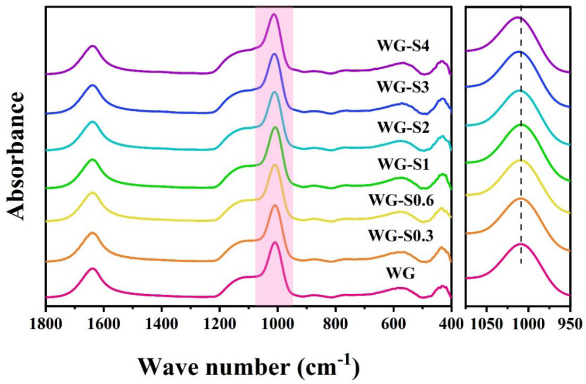

Figure 3. (a) Infrared absorption spectra of the tuned water glass solutions, (b) Enlarged view of the spectra over the wave number of 900-1125 cm^{-1}.

To investigate the effects of the SiO_2 addition on the water glass structure in detail, the absorption band at 1400-750 cm^{-1} in Figure 3 was deconvoluted, and the results are shown in Figure 4. According to the literature, there are mainly four absorption bands existing within this wavenumber range. The absorption band in the 1250-950 cm^{-1} region is composed of the superposition of three absorption bands located at ~1152 cm^{-1}, ~1066 cm^{-1} and ~1008 cm^{-1}, corresponding to the asymmetric stretching vibrations of (H)O-Si-O(H), Si-O-Si and (Na)O-Si-O(Na), respectively. When the amount of SiO_2 added is from 0.3 g to 4 g, the relative ratio of the absorption band corresponding to (Na)O-Si-O(Na) decreases from 42.3 % to 32.3 %, and the absorption band corresponding to (H) O-Si-O(H) increases slightly from 12.8 % to 14.3 %. The results suggest that the newly formed silica species were more coordinated and charge compensated by H^+ than Na^+. In addition, the proportion of the absorption band corresponding to Si-O-Si increases from 44.9 % to 53.5 %. This increase was mainly due to the dissolution of the added SiO_2 powder.

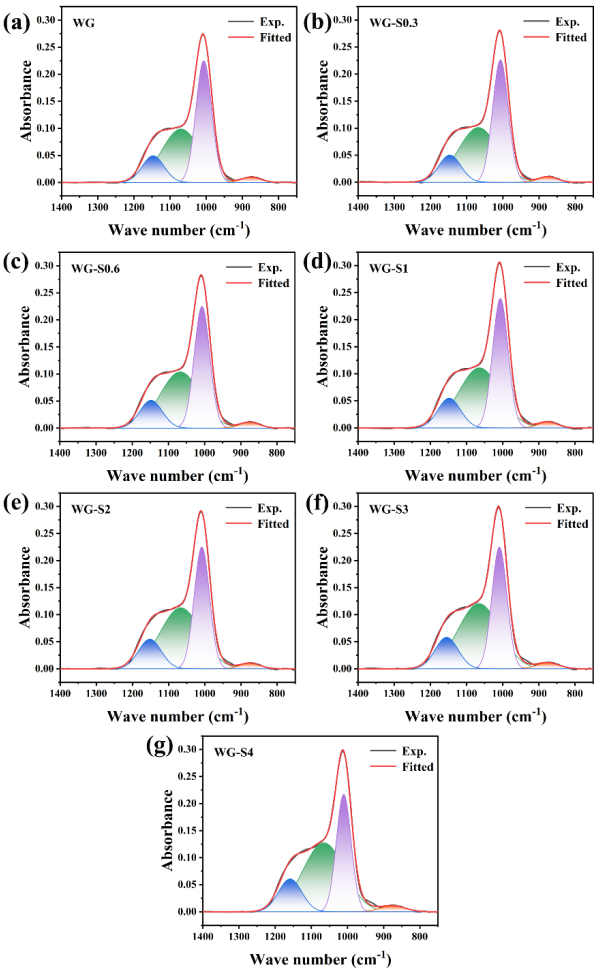

Figure 4. (a-g) Deconvolution of the infrared absorption bands over 1450-750 cm^{-1} of the tuned water glass solutions.

The ^{29}Si NMR spectra of the tuned water glass solutions are shown in Figure 5. The modified water glass still contains six distinct [SiO_4] structural units: Q^0, Q^1, Q^{2C}, Q^2, Q^3, and Q^4. Specifically, Q^0 represents monomeric [SiO_4]; Q^1 and Q^{2C} correspond to dimeric tetrahedra and cyclic structures, respectively; Q^2 and Q^3 are correlated with chain structures; and Q^4 represents fully polymerised silicate anions [21-23]. These units correspond to resonance peaks at chemical shifts of -71.2, -79.6, -81.9, -88.0, -96.8, and -106.1 ppm in the spectra, respectively.

As the amount of added SiO_2 increases, the Q^2 group in the tuned water glass shifts from -88.0 ppm to -88.4 ppm, the Q^3 group from -96.8 ppm to -97.4 ppm, and the Q^4 group from -106.1 ppm to -107.6 ppm. These shifts are associated with the degree of protonation of the silicon atoms. The degree of protonation of silicon atoms, i.e., the number of hydrogen atoms bonded to silicon,

depends on the pH value of the solution [24]. Water glass with a higher modulus has a lower pH, resulting in a higher degree of protonation. As the modulus of water glass increases, silicic acid undergoes polymerisation, leading to the formation of cyclic silicates. This is reflected in the spectrum by the enhancement of the Q^2, Q^3, and Q^4 peaks, along with the weakening of the Q^1 and Q^{2C} peaks. However, increasing the modulus has little effect on the Q^0 group. In high-modulus solutions, a significant portion of silicon atoms exist in the form of Q^4 species. The presence of highly polymerised silicate species was mainly contributed by the dissolved colloidal silica particles in the solution.

To confirm the above assumption, an analysis of the infrared spectrum and the ^{29}Si NMR spectrum of the porous SiO_2 powder added to the tuned water glass solutions was performed. As shown in Figure 6a, the absorption bands at 3426 cm^{-1} and 1635 cm^{-1} were attributed to the OH stretching vibration of the adsorbed water/silanol group and the OH bending vibration of the adsorbed water, respectively [25]. The absorption bands at ~1105 cm^{-1}, ~960 cm^{-1}, ~798 cm^{-1} and ~472 cm^{-1} correspond to the asymmetric stretching vibration of Si-O-Si, the asymmetric stretching vibration of Si-OH, the symmetric stretching vibration of Si-O-Si and the bending vibration of Si-O-Si, respectively [19, 25].

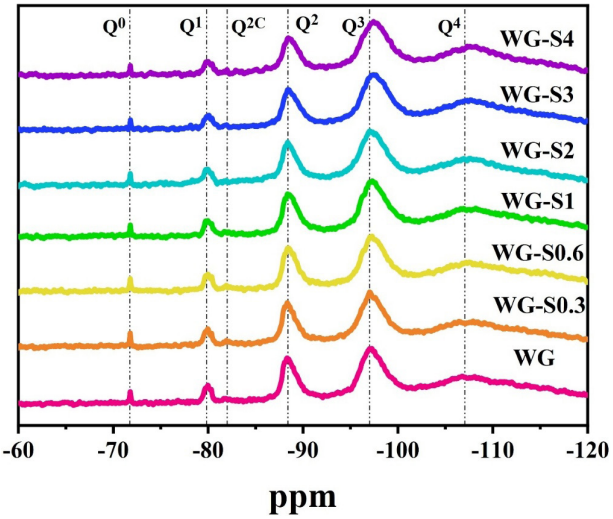

Figure 5. The ^{29}Si NMR spectra of the tuned water glass.

As shown in Figure 6b, the silica powder contains three different structural [SiO_4] units, namely the Q^2, Q^3, and Q^4 groups. The chemical shifts corresponding to these three structural units in the NMR spectrum are -87.4 ppm, -96.7 ppm, and -107.2 ppm, respectively [26]. A comparative analysis of the NMR spectra of pure SiO_2 (Figure 6b) and the tuned water glass solutions (see Figure 5) reveals that when the SiO_2 powder was added to the water glass, the content of the highly polymerised silicate anion groups Q^4 increases, while the amount of small molecular silica species remains largely unchanged. The results suggest that the added SiO_2 dissolved only to a limited extent, and its dissolution at the moderate synthesis conditions applied here was significantly weaker than that of the silicate framework existing in the Na_2O-SiO_2 binary glass frit originally used for the preparation of the precursor water glass. Therefore, although powder silica was apparently dissolved, its [SiO_4] skeleton was largely preserved in the tuned water glass solutions.

CONCLUSIONS

The modulus of water glass solution was easily and successfully tuned to be higher by dissolving porous silica powder in a commercial water glass solution

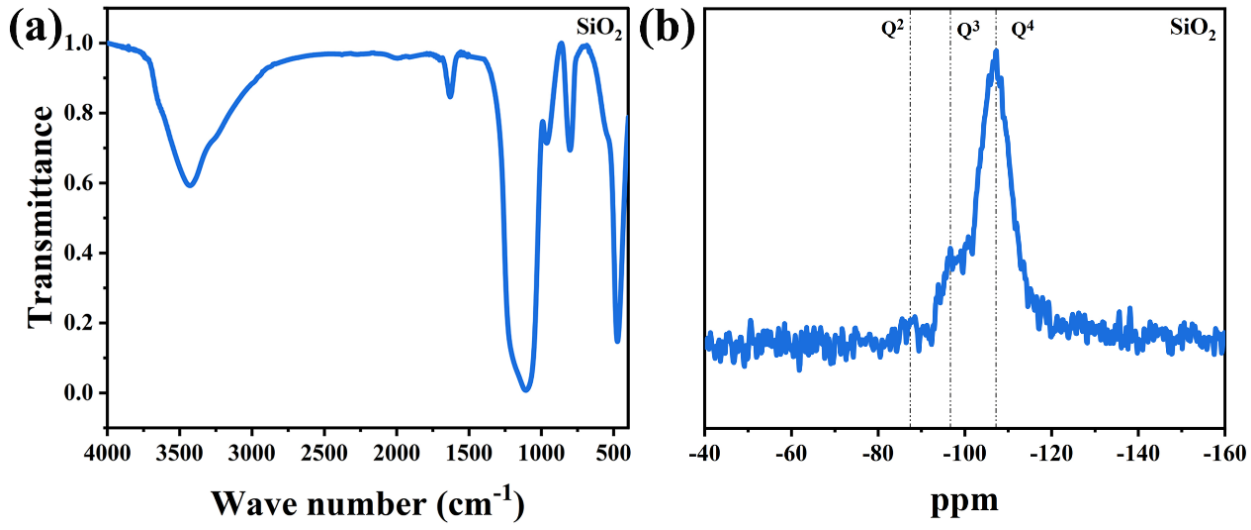

Figure 6. (a) Infrared spectrum and (b) ^{29}Si NMR spectrum of the SiO_2-added to increase the modulus of water glass solutions.

under stirring at 80 °C for 1.5 h. It was revealed that the water glass with a high modulus has a higher content of polymerised silica species (e.g., Q^4 structural units) due to the partially preserved silica skeleton of the dissolved silica. This structural variation explained the decreases in pH and conductivity, while it also explained the increase in viscosity of the tuned solutions.

Acknowledgements

This work was supported by the National Natural Science Foundation of China (No. 52272301).

REFERENCES

1. Sharmila G., Jeyalakshmi R. (2024): Unravelling the stability of solvated silicate species in sodium silicate activator solution of different silica modulus by FTIR and NMR studies and their chemical reactivity on metakaolin and fly ash geopolymerisation. *Sustainable Chemistry and Pharmacy, 39*, 101578. doi: 10.1016/j.scp.2024.101578
2. Seghir B. B., Hemmami H., Hocine B. M. E., Soumeia Z., et al. (2023): Methods for the Preparation of Silica and Its Nanoparticles from Different Natural Sources. *Biological Trace Element Research, 201*, (12) 5871-5883. doi: 10.1007/s12011-023-03628-w
3. Liu S., Ott W. K. (2020): Sodium silicate applications in oil, gas & geothermal well operations. *Journal of Petroleum Science and Engineering, 195*, 107693. doi: 10.1016/j.petrol.2020.107693
4. Febriana E., Mayangsari W., Yudanto S. D., Sulistiyono E., et al. (2024): Novel method for minimizing reactant in the synthesis of sodium silicate solution from mixed-phase quartz-amorphous SiO_2. *Case Studies in Chemical and Environmental Engineering, 9*, 100656. doi: 10.1016/j.cscee.2024.100656
5. Glück J., Dommaschk T., Jüngst D., Arimont J., et al. (2025): Thermoanalytical Investigation of the Curing Kinetics of Sodium Silicate as an Inorganic Binder for 3D Sand Printing. *Materials, 18*, (3) 667. doi: 10.3390/ma18030667
6. Mohamed Ismail A. A., Kannadasan K., Pichaimani P., Arumugam H., Muthukaruppan A. (2020): Synthesis and characterisation of sodium silicate from spent foundry sand: Effective route for waste utilisation. *Journal of Cleaner Production, 264*, 121689. doi: 10.1016/j.jclepro.2020.121689
7. Tong K. T., Vinai R., Soutsos M. N. (2018): Use of Vietnamese rice husk ash for the production of sodium silicate as the activator for alkali-activated binders. *Journal of Cleaner Production, 201*, 272-286. doi: 10.1016/j.jclepro.2018.08.025
8. Zhao W., Chang J., Wei Q., Wu J., Ye C. (2024): Effect of sodium silicate solution combined yttrium oxide stabilized zirconia nanopowders on the properties of alumina ceramics fabricated by binder jetting additive manufacturing. *Journal of Materials Processing Technology, 330*, 118454. doi: 10.1016/j.jmatprotec.2024.118454
9. Matinfar M., Nychka J. A. (2023): A review of sodium silicate solutions: Structure, gelation, and syneresis. Advances in *Colloid and Interface Science, 322*, 103036. doi: 10.1016/j.cis.2023.103036
10. Shao L, Yi M., Wei H., Ji R., He L., Jiang Y., Wang K. (2025): Synthesis of sodium silicate-activated metakaolin geopolymer microspheres (SS@MGMs) for efficient F^- removal from acidic wastewater. *Applied Clay Science, 276*, 107958. doi: 10.1016/j.clay.2025.107958
11. Yuan M.-r., Lu J.-t., Kong G. (2010): Effect of SiO_2:Na_2O molar ratio of sodium silicate on the corrosion resistance of silicate conversion coatings. *Surface and Coatings Technology, 204*, (8) 1229-1235. doi: 10.1016/j.surfcoat.2009.10.024
12. Veeraraghavan B., Haran B., Slavkov D., Prabhu S., et al. (2003): Development of a Novel Electrochemical Method to Deposit High Corrosion Resistant Silicate Layers on Metal Substrates. *Electrochemical and Solid-State Letters, 6*, (2) B4. doi: 10.1149/1.1537092
13. Qu J., Zhang J., Li H., Li (2021): A high value utilization process for coal gasification slag: Preparation of high S. modulus sodium silicate by mechano-chemical synergistic activation. *Science of The Total Environment, 801*, 149761. doi: 10.1016/j.scitotenv.2021.149761
14. Qu J., Zhang J., Li H., Li S., et al. (2024): Coal gasification slag-derived highly reactive silica for high modulus sodium silicate synthesis: Process and mechanism. *Chemical Engineering Journal, 479*, 147771. doi: 10.1016/j.cej.2023.147771
15. Chang J. J. (2003): A study on the setting characteristics of sodium silicate-activated slag pastes. *Cement and Concrete Research, 33*, (7) 1005-1011. doi: 10.1016/S0008-8846(02)01096-7
16. Luukkonen T., Sreenivasan H., Abdollahnejad Z., Yliniemi J., et al. (2020): Influence of sodium silicate powder silica modulus for mechanical and chemical properties of dry-mix alkali-activated slag mortar. *Construction and Building Materials, 233*, 117354. doi: 10.1016/j.conbuildmat.2019.117354
17. Lian X., Peng Z.-h., Shen L.-t., Qi T.-g., et al. (2021): Properties of low-modulus sodium silicate solution in alkali system. *Transactions of Nonferrous Metals Society of China, 31*, (12) 3918-3928. doi: 10.1016/s1003-6326(21)65774-6
18. Gao X., Zhou Q., Wang Y., Qi T., et al. (2023): Coal fly ash resource utilization: Structure of siloxy group of high-modulus sodium silicate solution. *Process Safety and Environmental Protection, 171*, 396-404. doi: 10.1016/j.psep.2023.01.022
19. Liu H., Kaya H., Lin Y. T., Ogrinc A., Kim S. H. (2021): Vibrational spectroscopy analysis of silica and silicate glass networks. *Journal of the American Ceramic Society, 105*, (4) 2355-2384. doi: 10.1111/jace.18206
20. Halasz I., Agarwal M., Li R., Miller N. (2007): Vibrational spectra and dissociation of aqueous Na_2SiO_3 solutions. *Catalysis Letters, 117*, (1-2) 34-42. doi: 10.1007/s10562-007-9141-6
21. Vidal L., Joussein E., Colas M., Cornette J., et al. (2016): Controlling the reactivity of silicate solutions: A FTIR, Raman and NMR study. *Colloids and Surfaces A: Physicochemical and Engineering Aspects, 503*, 101-109. doi: 10.1016/j.colsurfa.2016.05.039
22. Bass J. L., Turner G. L. (1997): Anion Distributions in Sodium Silicate Solutions. Characterization by 29SI NMR and Infrared Spectroscopies, and Vapor Phase Osmometry.

The Journal of Physical Chemistry B, 101, (50) 10638-10644. doi: 10.1021/jp9715282

23. Yuan M.-r., Lu J.-t., Kong G., Che C.-s. (2011): Effect of silicate anion distribution in sodium silicate solution on silicate conversion coatings of hot-dip galvanized steels. *Surface and Coatings Technology, 205*, (19) 4466-4470. doi: 10.1016/j.surfcoat.2011.03.064
24. Svensson I. L., Sjöberg S., Öhman L.-O. (1986): Polysilicate equilibria in concentrated sodium silicate solutions. *Journal of the Chemical Society, Faraday Transactions 1: Physical Chemistry in Condensed Phases, 82*, (12) 3635-3646. Doi: 10.1039/F19868203635
25. Ellerbrock R., Stein M., Schaller J. (2022): Comparing amorphous silica, short-range-ordered silicates and silicic acid species by FTIR. *Scientific Reports, 12*, 11708. doi: 10.1038/s41598-022-15882-4
26. Fait F., Steinbach J. C., Kandelbauer A., Mayer H. A. (2023): Incorporation of silica nanoparticles into porous templates to fabricate mesoporous silica microspheres for high performance liquid chromatography applications. *Journal of Chromatography A, 1705*, 464190. doi: 10.1016/j.chroma.2023.464190